Biosensors and Bioelectronics 178 (2021) 113033

Contents lists available at ScienceDirect

Biosensors and Bioelectronics

journal homepage: http://www.elsevier.com/locate/bios

μDrop: Multi-analyte portable electrochemical-sensing device for blood-based detection of cleaved tau and neuron filament light in traumatic brain injury patients

Sultan Khetani [a,b,1], Anupriya Singh [a,b,1], Brendon Besler [c,2], Savitri Butterworth [c,2], Thomas Lijnse [b,2], Kenneth Loughery [c,2], Katrin Smith [c,2], Ehsan Hosseini [d], Rakesh Narang [a,b], Kunal Karan [d], Chantel Debert [g,h], Arindom Sen [b,d,e,f], Kartikeya Murari [b,c], Amir Sanati- Nezhad [a,b,e,*]

[a] BioMEMS and Bioinspired Microfluidic Laboratory, Department of Mechanical and Manufacturing Engineering, University of Calgary, Calgary, Alberta, T2N 1N4, Canada
[b] Biomedical Engineering Graduate Program, University of Calgary, Calgary, Alberta, T2N 1N4, Canada
[c] Department of Electrical and Computer Engineering, Schulich School of Engineering, University of Calgary, Calgary, Alberta, T2N 1N4, Canada
[d] Department of Chemical and Petroleum Engineering, University of Calgary, Calgary, Alberta, T2N 1N4, Canada
[e] Center for Bioengineering Research and Education, Schulich School of Engineering, University of Calgary, Calgary, Alberta, T2N 1N4, Canada
[f] Pharmaceutical Production Research Facility, Schulich School of Engineering, University of Calgary, Calgary, Alberta, T2N 1N4, Canada
[g] Department of Clinical Neurosciences, Hotchkiss Brain Institute, Alberta Children Hospital Research Institute for Child and Maternal Health, University of Calgary, Calgary, Alberta, T2N 1N4, Canada
[h] Department of Clinical Neurosciences, Division of Physical Medicine and Rehabilitation, Foothills Medical Centre, University of Calgary, Calgary, Alberta, T2H 2T9, Canada

ARTICLE INFO

Keywords:
Traumatic brain injury (TBI)
Cleaved-tau protein (C-Tau)
Neuron filament protein (NFL)
Electrochemical immuno-biosensor
Biomedical device

ABSTRACT

Over 27 million individuals are affected every year worldwide with central nervous system (CNS) injuries. These injuries include but are not limited to traumatic brain injury (TBI) and spinal cord injury (SCI). CNS injuries remain a significant public health concern which demands reliable tools for rapid, on-sight, on-field, and point-of-care diagnostic (POC) solutions. To address these challenges, we developed a low-cost, open-source, hand-held, portable, and POC detection technology, termed as MicroDrop (μDrop), which can simultaneously detect up to eight target biomolecules and display results in both analog and digital formats. The data acquired is stored wirelessly in a cloud server for further investigation and statistical analysis. Multiplexing capability of μDrop and immuno-biosensors detects and quantifies Cleaved-Tau Protein (C-Tau) and Neuron-Filament (NFL) proteins in the blood of TBI patients. Immuno-biosensors rapidly sense the two target proteins in less than 30 min, with μDrop and a conventional potentiostat. C-Tau and NFL were selectively detected with μDrop within the dynamic range of 10 pg/mL - 100 ng/mL and the sensitivity range of 47 μA/pg mm^2 - 65 μA/pg mm^2. Comparing the biosensing performance with enzyme-linked immunosorbent assays (ELISA) shows that the immuno-biosensors combined with μDrop could successfully differentiate between clinical controls and injured patients.

1. Introduction

Each year, more than 27 million individuals globally suffer from traumas to the brain, and spinal cord, collectively referred to as central nervous system (CNS) injuries (James et al., 2019). In North America, over 5.3 million CNS injuries are registered due to violence, falls, vehicular accidents, and sports-related injuries (James et al., 2019; Langlois et al., 2006; Rao et al., 2017). Annual global economic expenditure is exceeding $400 billion in direct and indirect expenses. These expenses include hospitalization, diagnostic testing,

* Corresponding author. Department of Mechanical and Manufacturing Engineering, 2500 University Drive NW, Calgary, Alberta, T2N 1N4, Canada.
E-mail address: amir.sanatinezhad@ucalgary.ca (A.S. Nezhad).
[1] These are the first co-authors and contributed equally to the manuscript.
[2] These are the second co-authors and contributed equally to the manuscript.

https://doi.org/10.1016/j.bios.2021.113033
Received 25 November 2020; Received in revised form 18 January 2021; Accepted 20 January 2021
Available online 23 January 2021

rehabilitation, and productivity loss (Center 2010; Langlois et al., 2006; Organization and Society 2013; Peeters et al., 2015). Primary injuries to the brain include diffuse axonal injury, focal hemorrhage, and blood collection in the brain (hematoma) (North et al., 2012; Zetterberg et al., 2013). In such a condition for patients, rapid and frequent diagnostic tests can reduce morbidity and mortality associated with CNS injuries (Langlois et al., 2006; Levin and Diaz-Arrastia 2015; Li et al., 2010; North et al., 2012; Organization and Society 2013). Although computed tomography (CT) and magnetic resonance imaging (MRI) are current clinical gold standards for the diagnosis and prognosis of CNS injury, they are not suitable for point-of-care (POC) applications. Moreover, they are often not available at rural and remote locations, lack portability, have a high cost of operation and testing, and cause excessive exposure to radiation when frequently used (Doolan et al., 2012; North et al., 2012; Organization and Society 2013). Therefore, the ability to rapidly test, detect, and diagnose CNS injuries and frequently monitor injury status remains a major unmet clinical need.

An alternative to neuroimaging techniques and questionnaire-based tests measures the concentration of protein biomarkers released in bodily fluids (North et al., 2012). Several CNS-based blood protein biomarkers, such as S100 calcium-binding protein β (S100β), glial fibrillary acidic protein (GFAP), and ubiquitin C-terminal hydrolase L1 (UCHL-1) are released after a CNS injury (Khetani et al., 2017a; Khetani et al. 2018b, 2019). Cleaved Tau (C-Tau) and Neuron filament light protein (NFL) were selected for this study, as they are known to be the primary molecular indicators of axonal injury. C-Tau is an early indicator of TBI, with concentrations rising from a baseline of <70 pg/mL, peaking within 6 h up to 1700 pg/mL – 8700 pg/mL (Adrian et al., 2016; North et al., 2012; Zetterberg et al., 2013). On the other hand, NFL concentration increases from <35 pg/mL to a peak concentration of 2000 pg/mL – 10,000 pg/mL after 4 – 10 days post-injury (Adrian et al., 2016; North et al., 2012; Zetterberg et al., 2013). Although the elevated levels would be ideal for detecting TBI, the small change of concentrations for mTBI and concussion necessitates biosensors with the limit of detection (LOD) of tens of pg/mL (Adrian et al., 2016; North et al., 2012).

Although enzyme-linked immunosorbent assays (ELISA) quantifies proteins (Gorodkiewicz et al., 2011; North et al., 2012), its workflow is developed for processing a large number of samples. They also require several sample-preparation steps, designated infrastructure, and trained operators for full functionality. Although sensitive immuno-biosensors detecting biomarkers within 1 ng/mL to 1 mg/mL range are reported (del Río et al., 2019; Khetani et al., 2017a; Khetani et al. 2019; Khetani et al. 2018b; Safavieh et al., 2017; Safavieh et al., 2016; Salahandish et al., 2018a; Salahandish et al. 2018b; Salahandish et al., 2019a; Salahandish et al. 2018c; Salahandish et al. 2019b), this concentration still do not fall within the range and LOD change detecting TBI (North et al., 2012). Although high-resolution ELISAs from Quanterix detect TBI biomarkers within 10 fg/mL to 100 ng/mL range, they are not suitable for POC applications (Gill et al., 2018; Mohammadian et al., 2019; Wang et al., 2018).

Among all immuno-biosensors, electrochemical biosensors offer a highly linear detection range, low LOD, and rapid measurement due to factors, including label-free sensing and quantitative electrical output (Bruch et al., 2019; Du et al., 2020a; Singh et al., 2017). Moreover, the surface chemistry, possibility to add nanomaterial coatings on the electrode, enhances the electrical conductivity and thereby the sensitivity in detection (Khetani et al. 2019, 2020a, 2020b; Salahandish et al., 2019b). While nano-biosensors are miniaturized and compatible with POC applications, most of the electrochemical immuno-biosensors use benchtop potentiostats (Khetani et al., 2018a, 2019; Salahandish et al., 2019b; Valente et al., 2017; Vedadghavami et al., 2017). Although newer designs of potentiostats have been reported, their curve-shaped output reading is not universally understood, requires further data processing and interpretations, and complicates the practical implementation of electrochemical immuno-biosensors for POC applications (Ainla et al., 2018; Dryden and Wheeler 2015; Rowe et al., 2011).

Here, we developed a new sensing platform, called MicroDrop (μDrop), to overcome the barriers to rapid and accurate CNS injuries detection (Scheme 1). μDrop addresses the key limitations of readout systems that utilize electrochemical immuno-biosensors for biosensing applications. Using μDrop in conjunction with electrochemical immune-biosensors, offers a highly intuitive, low-cost, sensitive, portable, and sensitive detection system of multiple CNS injury proteins fit for POC applications. While several different electrochemical techniques such as impedance spectroscopy (EIS) (Khetani et al. 2017b, 2018b) and square wave voltammetry (SWV) (Khetani et al., 2019) have been implemented, this work used differential pulse voltammetry (DPV) in conjunction with μDrop to create a compact sensing unit. Given its ability to cancel the background signal, DPV offers high sensitivity to potential and current, enabling the detection of electroactive species at low concentrations. DPV current response decreases for the increased antigen concentration, resulting from the inactive antigen-antibody complex on the immunosensors' surface (Mo and Ogorevc 2001). This implementation increases the measurable range of analytes down to parts per billion in complex bodily fluids like the blood (Molina and González 2016; Osteryoung et al., 1981). μDrop and immuno-biosensors enabled the detection and quantification of C-Tau and NFL in pg/mL concentration range for both lab-prepared and clinical blood samples within <30 min and costing <$20/test.

2. Methods

2.1. Creation of the immuno-biosensor

The details of the μDrop development are presented in Supplementary Information **SI – 1**. Electrodes were fabricated using a magnetron sputtering technique. The electrodes' geometry was created from polymethyl methacrylate (PMMA) shadow masks for patterning the electrodes. Details of the sputtering, electrode geometry, shadow masks, functionalization of electrodes, antibody immobilization, detection of C-Tau and NFL proteins, and ELISA protocol are presented in **SI – 1K**. Using this technique, 10 electrodes were produced on a single glass slide (Fig. S1JA). The microfluidic chip (shown in Fig. S1JB) was designed such that it can be used for multiplexed measurement.

3. Results and discussion

3.1. μDrop design, fabrication, and operation

μDrop design contains a readout system and a biosensing unit. The readout system works as a miniaturized potentiostat. It measures the redox current of the biosensor strip through the DPV technique and operates within a specific pre-set detection range (**Figure S 1A).** The electrochemical reaction, initiated by the DPV, produces an electrical current through the counter electrode (CE), followed by measuring the current between the CE and working electrode (WE) and correlating it with the analyte concentration (Khetani et al., 2017a). Eight identical DPV modules were used to allow the measurement of eight parallel sensing channels. Each module consists of a potentiostat controlled by a small "slave" microcontroller to apply a voltage and convert the resulting response into a digital signal. The "slave" then communicates with the "master" microcontroller, which coordinates the slaves, manages data transfers, and monitors user inputs. Details and circuit diagrams of potentiostat circuits, slave microcontrollers, power module, data storage, display, and the user interface are shared in the supplementary file (**SI – 1**).

3.2. Comparison between μDrop and a commercial potentiostat

The working of the μDrop was benchmarked with a commercial potentiostat (PGSTAT, Metrohm Autolab, Ontario). The standard redox

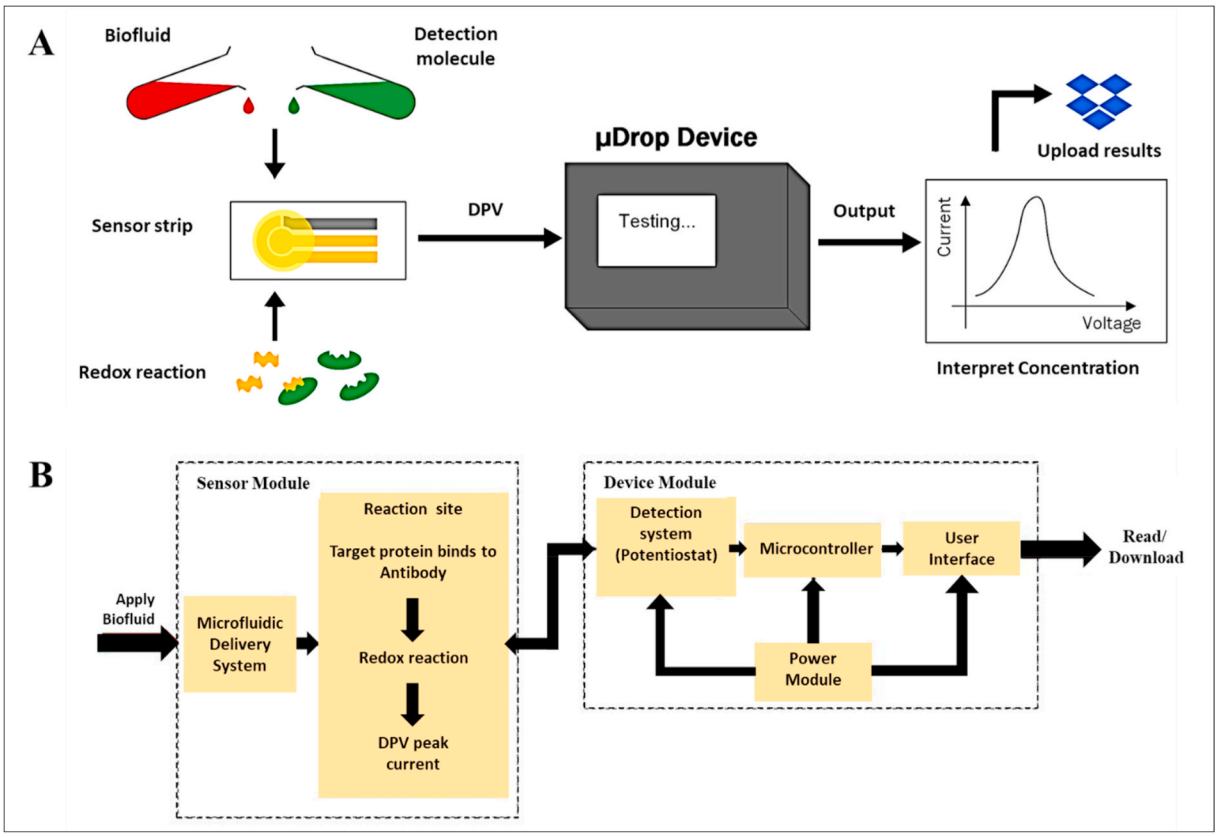

Scheme 1. Representation of the concept and the working principle of the MicroDrop (µDrop) platform. (**A**) Overview of the working principle of the µDrop. The self-assembled monolayer (SAM) surface modification technique converts fabricated electrodes to biosensors. The biofluid containing the target biomarkers binds to the respective antibodies. µDrop initiates differential pulse voltammetry (DPV) signal, which triggers a redox reaction. The DPV signal is displayed on the device, and the data file is stored in a cloud-based data storage module. (**B**) The overview of the biosensing modules of the µDrop. The sensing module undergoes a redox reaction where it is triggered to record a DPV signal. The readout module contains a multichannel potentiostat circuit, a power system, and a user interface, which synchronously manages the reactions on the biosensing module. Microcontrollers were programmed to control the electronic protocols, experimental processes, display, output, and data storage in a cloud-based app.

probe $[K(Fe(CN)_6]^{3-/4-}$ within a concentration range of 1 mM – 5 mM were tested with both devices. A close correlation was observed between DPV current peaks generated for each concentration of the redox probe was found with both devices ($>R^2 = 0.99$) (Fig. 1 A, SI - 2). The results showed that the output of the µDrop offers the same precision of detection as the commercial potentiostat. Besides µDrop offering precision, reproducibility, portability, and multiplexing detection, the coefficient of variations (COVs) for three repetitive measurements with the µDrop was <4.3%, whereas the COVs for the commercial potentiostat was <4.1%. The µDrop manages 8-parallel measurements and has a much smaller form factor (size: 5.5 × 2.5 × 2.4 cm^3, weight: 0.35 kg) compared to the PGSTAT204 commercially available benchtop potentiostat (size: 9 × 21 × 15 cm^3, weight: 2.1 kg). Furthermore, the µDrop is more cost-effective and affordable with a price of $680/unit (Table S1D) compared to a fully functional single-channel benchtop potentiostat, such as PGSTAT204, which is priced above $6000 (Ainla et al., 2018). An additional comparison between the µDrop and a few similar portable detection devices is shown in Table S2. The µDrop's readout system performs well compared to similar devices given its functionality, user interface, multiplexing option, and diagnostic capability.

3.3. Surface chemistry of the immuno-biosensors

3.3.1. Confirmation of the functional groups

The surface of the working electrode is modified using a self-assembled monolayer (SAM), which converts the electrode into a biosensor. Details of the electrode's surface modification are given in **SI – 1K**. The SAM and antibodies' presence were confirmed by determining the functional groups using Fourier transform spectroscopy-attenuated total reflection (FTIR-ATR) (**SI - 3**). The FTIR peaks specific to 11-Mercaptoundecanoic acid (MUA) were observed at 1697 cm^{-1} for carboxylic groups (C = = O), and 2850 cm^{-1} and 2918 cm^{-1} for alkyl chains (CH_2) (Fig. S3A) (Šimšíková et al., 2013). The absorbance spectra at 1536 cm^{-1} and 1642 cm^{-1} confirmed –CH_2 asymmetric stretching vibration, and C = = O vibrations belonged to the amide group of the linker EC-NHS (Fig. S3B) (Xiong et al., 2017). Characteristic absorbance peaks at 1239 cm^{-1}, 1496 cm^{-1}, 1600 cm^{-1}, and 1660 cm^{-1} were observed on NFL-antibody modified electrodes. Absorbance peaks between 1300 cm^{-1} and 1500 cm^{-1} are attributed to the CH_2 and CH_3 groups in the glycine component. Strong peaks at 1585 cm^{-1} and 1600 cm^{-1} are attributed to the –NH_2 groups in antibody's amino acids (Fig. S3C) (Boulet-Audet et al., 2016). These characteristic peaks belonging to the SAM and antibody immobilization confirmed the completion of converting a bare electrode into a functional immuno-biosensor.

3.3.2. Morphology visualization of the immuno-biosensors

Atomic force microscopy (AFM) was used to identify the morphology of all surface modification steps during the preparation of the immuno-biosensors. The morphology of the bare (uncoated) electrode and the SAM modified electrodes was nearly the same, and the height of the modified surface remained between 1 nm and 2 nm (Fig. 1 B-D). The NFL antibody-immobilized electrode shows a typical globular structure on the surface of the electrode. The roughness of the antibody-immobilized

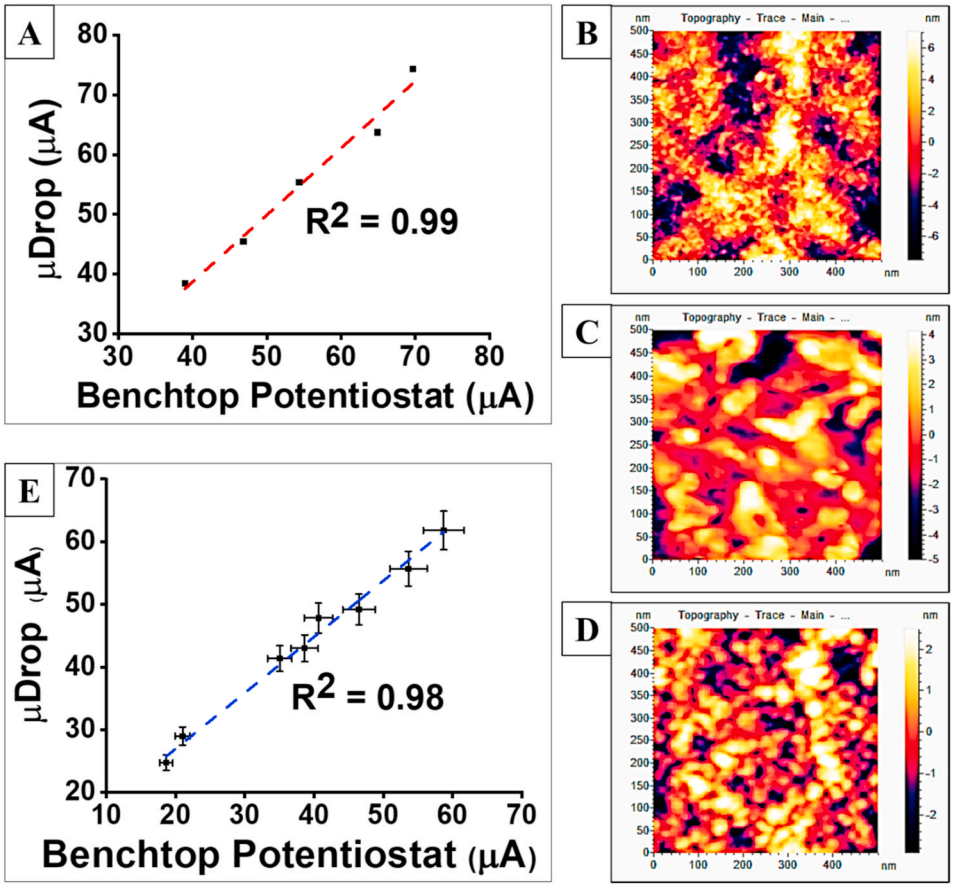

Fig. 1. The performance of the μDrop's readout system compared to a commercial potentiostat, and the morphology visualization of the immuno-biosensors. (**A**) Comparison between the DPV current peaks obtained from μDrop and a benchtop potentiostat in the presence of 1 mM–5 mM redox probes. (**B-D**) Morphology characterization of the immuno-biosensor was analyzed by an atomic force microscope (AFM) to assess the success of the surface modification steps: (**B**) Blank or un-coated Gold (Au)/Chrome (Cr) electrode, (**C**) Au electrode modified with 11-Mercaptoundecanoic acid (MUA) and cross-linked with N-(3-Dimethylaminopropyl)-N′-ethylcarbodiimide hydrochloride - N-hydroxysuccinimide (EDC-NHS), created a self-assembled monolayer (SAM), and (**D**) Neuron filament light (NFL)-antibody immobilized biosensor. (**E**) The comparison of DPV electrochemical characterization peak currents performed after every step of electrode modification with the μDrop and a benchtop potentiostat in the presence 4 mM redox probes (n = 3). Peak currents for Blank, SAM, Antibody-NFL, antibody-C-Tau, BSA/blocking on NFL, BSA/blocking on C-Tau, 10 ng/mL NFL, 10 ng/mL C-Tau are shown. All measurements were performed three times (n = 3), and the data is displayed as mean ± SEM. (For interpretation of the references to colour in this figure legend, the reader is referred to the Web version of this article.)

electrode increases from approximately 2 nm to above 4 nm, confirming the presence of antibodies immobilized on the surface (Fig. 1D).

3.3.3. *Diffusion kinetics of the immuno-biosensors*

The diffusion kinetics of the SAM-modified electrodes was assessed by measuring the cyclic voltammetry (CV) scan rate on the redox current with a commercial potentiostat. The SAM performance was examined in the presence of 4 mM redox probes with CV scan rates ranging from 10 mV s^{-1} to 100 mV s^{-1}. The results showed that the peak redox current increased linearly with an increase in scan rate, and the distance between the peaks widens (Fig. S4A). The linear fit between the oxidation peak current (Ipa) and the reduction peak current (Ipc) was related to the square root of the scan rate ($v^{1/2}$). Linear equations were identified as $Ipa = 0.0034\, v^{1/2} - 0.0057$ ($R^2 = 0.98$) and $Ipc = -0.008\, v^{\frac{1}{2}} + 0.0053$ ($R^2 = 0.98$) (Fig. S4B). The results confirmed that the electrochemical signal recorded was diffusion-controlled (Du et al., 2020b).

3.4. *Electrochemical characterization of the immuno-biosensors with the μDrop and a commercial potentiostat*

Conversion of the electrodes into immuno-biosensors was confirmed electrochemically by characterizing them via both μDrop and a benchtop potentiostat in the presence of 4 mM redox probe solution. The surface modification steps are detailed in the method section. Immuno-biosensors exhibited a decreasing DPV peak current when they were characterized by both the benchtop potentiostat and the μDrop (**SI 5**). DPV current responses from both the readout systems after each step of surface modification showed a comparable relationship between the peak currents. Upon measuring the signals with the benchtop potentiostat, the unmodified electrode offered a DPV peak current of 58.71 μA in the presence of a 4 mM redox probe (Fig. S5A). The peak current decreased to 53.62 μA upon the addition of the SAM (MUA + EDC-NHS). For the 25 μg/mL NFL and C-tau antibody immobilized electrodes, the peak current further decreased to 46.47 μA and 40.64 μA, respectively. Adding 0.25% bovine serum albumin (BSA) on NFL and C-Tau modified electrodes (to prevent non-specific binding on the biosensor) resulted in 38.64 μA and 35.04 μA DPV peak currents, respectively. Lastly, adding 10 ng/mL NFL and C-Tau antigens spiked in PBS resulted in 21.02 μA and 17.66 μA DPV peak currents, respectively (Fig. S5A).

Similar to the benchtop potentiostat measurement, the unmodified electrode showed a DPV peak current of 61.79 μA when measured with the μDrop (Fig. S5B). The peak current decreased to 55.68 μA upon the surface modification by SAM (MUA + EDC-NHS). The DPV peak current decreased further to 49.17 μA and 47.8 μA upon immobilizing 25 μg/mL NFL and C-tau antibodies, respectively, for each antibody. Adding BSA (0.25% in PBS) on the NFL and C-Tau antibody immobilized electrodes decreased the DPV peak current to 42.98 μA and 41.35 μA, respectively. Finally, C-Tau and NFL (10 ng/mL) proteins were added to the immuno-biosensors and incubated for 30 min decreased DPV peak currents to 28.97 μA and 24.73 μA, respectively.

The successive reduction in the DPV peak currents after each step of the surface modification can be attributed to non-conductive layers resulting in decreased diffusion of the redox probes on the working electrodes (Fig. S5A,B) (Khetani et al., 2017a). The comparison between the peak currents recorded at every step of the surface modification showed a coefficient correlation (R^2) of 0.98 at a 5% error rate (Fig. 1E). The results confirmed that the measurements recorded with both the commercial potentiostat and the μDrop had a close correlation. The μDrop is reliable for the sensitive detection of NFL and C-Tau biomarkers. Moreover, the decrease in the peak current had a considerable and discernible margin, implying detection thresholds are measurable by the μDrop similar to a benchtop potentiostat. Additionally, the

reproducibility test confirmed the reliability of the measurements by μDrop and the immuno-biosensors (Table S3A).

3.5. Analytical performance of the immuno-biosensors

3.5.1. Immuno-biosensors response measured by μDrop and a commercial potentiostat

The linear detection range of the immuno-biosensors was measured by testing within the C-Tau and NFL concentration range of 100 μg/mL - 100 fg/mL. The results showed a decreasing DPV response with an increase in the concentration of the target analytes. Both C-Tau and NFL were detectable within the range of 1 pg/mL to 1 μg/mL with the benchtop potentiostat. The dynamic detection range followed a linear correlation between the response electrical current (Y) and the analytes' concentrations (X). The correlation equation for the biosensor response to C-Tau was determined as $Y = 2.24 \times X - 0.347 (R^2 = 0.98)$. A similar response for NFL detection led to the equation: $Y = 3.79 \times X - 0.47$ ($R^2 = 0.98$) (Fig. 2 A, B).

On the other hand, C-Tau and NFL immuno-biosensors offered a similar linear response when tested with the μDrop within the concentration range of 1 pg/mL – 1 μg/mL of proteins spiked in PBS solution. The linear regression equation for C-Tau detection was determined to be $Y = 3.51 \times X - 0.82$ ($R^2 = 0.98$), and the linear regression for NFL detection was determined as: $Y = 3.03 \times X - 0.53$ ($R^2 = 0.98$) (Fig. 2 C, D). Unlike the commercial potentiostat, NFL and C-Tau were reliably detected down to 10 pg/mL concentration using the μDrop. The lower sensitivity of the μDrop compared to the commercial potentiostat may be design related, which showed lower resolution in detecting smaller variations between peak currents at the extreme concentrations of the analytes. Despite the small reduction in the detection range of the μDrop compared to the commercial potentiostat, the μDrop setup and immuno-biosensors operated well within the physiologically relevant levels of C-Tau and NFL needed for the diagnosis and monitoring of CNS injuries (Adrian et al., 2016; North et al., 2012; Yokobori et al., 2015).

The sensitivity and LOD of the C-Tau and NFL immuno-biosensors were evaluated based on their calibration responses. The sensitivity of an immuno-biosensor was calculated as $Sensitivity = m/A$, where m is the slope of its calibration plot, and 'A' is the geometrical surface area of the working electrode (Sha et al., 2017). While the surface area of all the immuno-biosensors was 25 mm^2, the slopes for each target analyte is unique. With the same surface area, the slope depends on the binding strength between the target analytes (here proteins) to their respective capture antibodies (Fig. 2). The sensitivity of the immuno-biosensors measured by the commercial potentiostat was determined to be 28.54 μA/pg mm^2 for detecting C-Tau and 48.28 μA/pg mm^2 for detecting NFL. Similarly, the sensitivity of the immuno-biosensors measured by μDrop was determined to be 44.71 μA/pg mm^2 for detecting C-Tau and 38.56 μA/pg mm^2 for NFL (Table S3B). The minimum concentration change detectable by the immuno-biosensors indicated by LOD was calculated as, $LOD = (3 \times Std.Dev)/m$ ($slope\ of\ the\ caliberation\ curve$) (Sha et al., 2017). The LOD of the immuno-biosensors was measured to be 0.34 pg/mL for C-Tau and 0.2 pg/mL for NFL when quantified by the commercial potentiostat. Similarly, the μDrop offered nearly the same sensitivity but with a superior LOD than the commercial potentiostat.

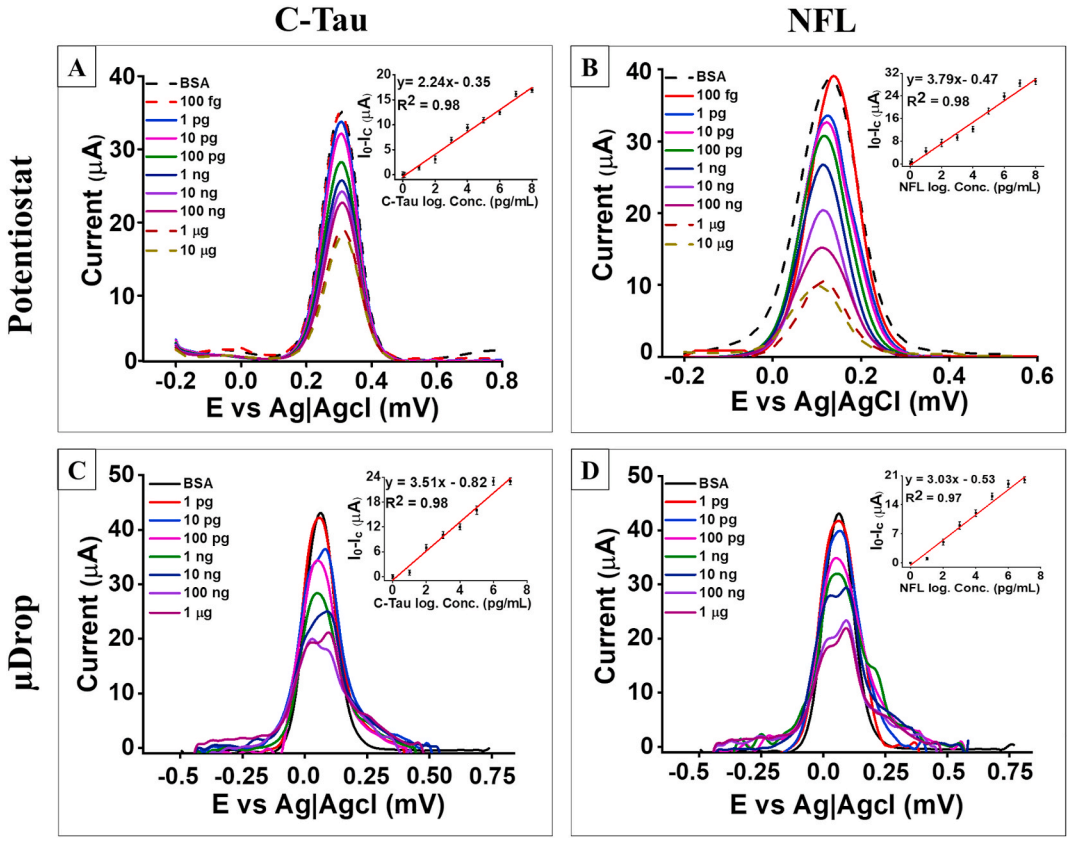

Fig. 2. The response of the immuno-biosensors to Cleaved-Tau protein (C-Tau) and Neuron Filament light (NFL) proteins measured by both a commercial potentiostat and the μDrop. The analytical performance of immuno-biosensors measured by a commercial benchtop potentiostat detecting 100 fg/mL - 10 μg/mL concentration of (**A**) C-Tau and (**B**) NFL. The detection range for both proteins detected by the commercial potentiostat was determined to be between 1 pg/mL – 1 μg/mL. The analytical performance of the immuno-biosensor measured by μDrop readout detecting 1 pg/mL - 10 μg/mL concentrations of **(C)** C-Tau and (**D**) NFL. The difference between the BSA-modified electrode (I_0) and C-Tau or NFL concentrations tested (Ic) was used as an analytical metric. The analytical range for both the C-Tau and NFL with the μDrop was determined to be within 10 pg/mL - 100 ng/mL. All measurements were performed three times (n = 3), and the data is displayed as mean ± SEM.

The LODs of the immuno-biosensors measured by the μDrop was 0.14 pg/mL for C-Tau and 0.16 pg/mL for NFL (Table S3B). The difference in the sensitivity and LOD between the C-Tau and NFL immuno-biosensors attributed to the molecular weights of C-Tau (335 kDa) and NFL (70 kDa), and the selectivity level of the capture antibodies for their respective analytes. Compared to NFL, the larger C-Tau molecules occupied a relatively larger surface area of the immuno-biosensor, which reduced the redox probe's diffusion toward the electrode. In summary, based on the comparative analysis of the operational detection range and sensing performance, μDrop and the biosensors developed in this work are qualified for point-of-care detection of the C-Tau and NFL protein biomarkers (Adrian et al., 2016).

3.6. Performance of the immuno-biosensors in PBS matrix

The biosensors' responses were measured with the benchtop potentiostat within the detectable range in PBS based on the above-described calibration curve. C-Tau and NFL were measured in PBS between 1 pg/mL - 1 μg/mL concentrations. For C-Tau, the response was measured as: $Y = 2.36 \times X - 0.86 (R^2 = 0.98)$, and for NFL, the response was measured: $Y = 4.14 \times X - 1.95$ ($R^2 = 0.97$), where 'Y' is the peak current and 'X' is the concentration of the target protein (Fig. S5A). The LOD and the sensitivity for detecting C-Tau were 0.32 pg/mL and 30.1 μA/pg mm^2, respectively. The LOD and the sensitivity for detecting NFL were 0.18 pg/mL and 52.7 μA/pg mm^2, respectively (Table S3B).

Given the comparable performance of the immuno-biosensors measured by the μDrop, the response of immuno-biosensors to C-Tau and NFL proteins were measured in the dynamic detection range of 10 pg/mL - 100 ng/mL concentrations in PBS. For C-Tau, the equation was calculated as follows: $Y = 3.71 \times X - 1.28$ ($R^2 = 0.96$). For the NFL, $Y = 3.51 \times X - 1.87$ ($R^2 = 0.98$) was found (Fig. 3 A, B; Fig. S5B). The LOD and the sensitivity of the biosensors for detecting C-Tau by the μDrop were 0.14 pg/mL and 47.3 μA/pg mm^2, respectively, and for NFL, they were 0.13 pg/mL and 64.7 μA/pg mm^2, respectively, in the PBS (Table S3B). Simultaneous C-Tau and NFL detection by μDrop was performed by mounting the microfluidic chip over the C-Tau and NFL immuno-biosensors. C-Tau and NFL samples were individually added toward their respective biosensors. The multiplex detection of C-Tau and NFL did not change the performance of the μDrop and the outcomes of the biosensors. The LOD, detection range and linear correlation remained the same as observed for a single target, demonstrating the reliability of the μDrop sensing platform's reliability for multiplexed immuno-biosensing.

3.7. Performance of the immuno-biosensors in serum measured by the μDrop's readout system

The response of C-Tau and NFL immuno-biosensors measured by the μDrop readout system was assessed by spiking C-Tau and NFL proteins in healthy human blood serums. Based on the detection range obtained in PBS, C-Tau and NFL were spiked within the concentration range of 10 pg/mL to 100 ng/mL in human serums, and the responses of the immuno-biosensors were recorded. A linear response similar to biosensors' responses in the PBS was observed within the human serum. The detection range of both the immuno-biosensors for target analytes in serum remained between 10 pg/mL – 100 ng/mL, the same as that in PBS. The linear dynamic relation between the DPV peak current (Y) and the target's concentration (X) was determined to be: $Y = 5.08 \times X - 3.21 (R^2 = 0.99)$ (Fig. 3C). A similar relationship was detected for the NFL as: $Y = 4.21 \times X - 6.21 (R^2 = 0.97)$ (Fig. 3D). The sensitivity and LOD for C-Tau were determined to be 0.1 pg/mL and 64.72 μA/pg mm^2, respectively. Similarly. for NFL analyte, they were 0.11 pg/mL and 53.63 μA/pg mm^2, respectively, in the serum (Table S3B). The performance of the immuno-biosensors measured by the μDrop in identifying and quantifying the target C-Tau and NFL analytes within a complex matrix like serum confirms the utility of the μDrop sensing platform for testing clinical samples. Furthermore, the developed immune-biosensors vastly outperformed all other published reports when comparing linear

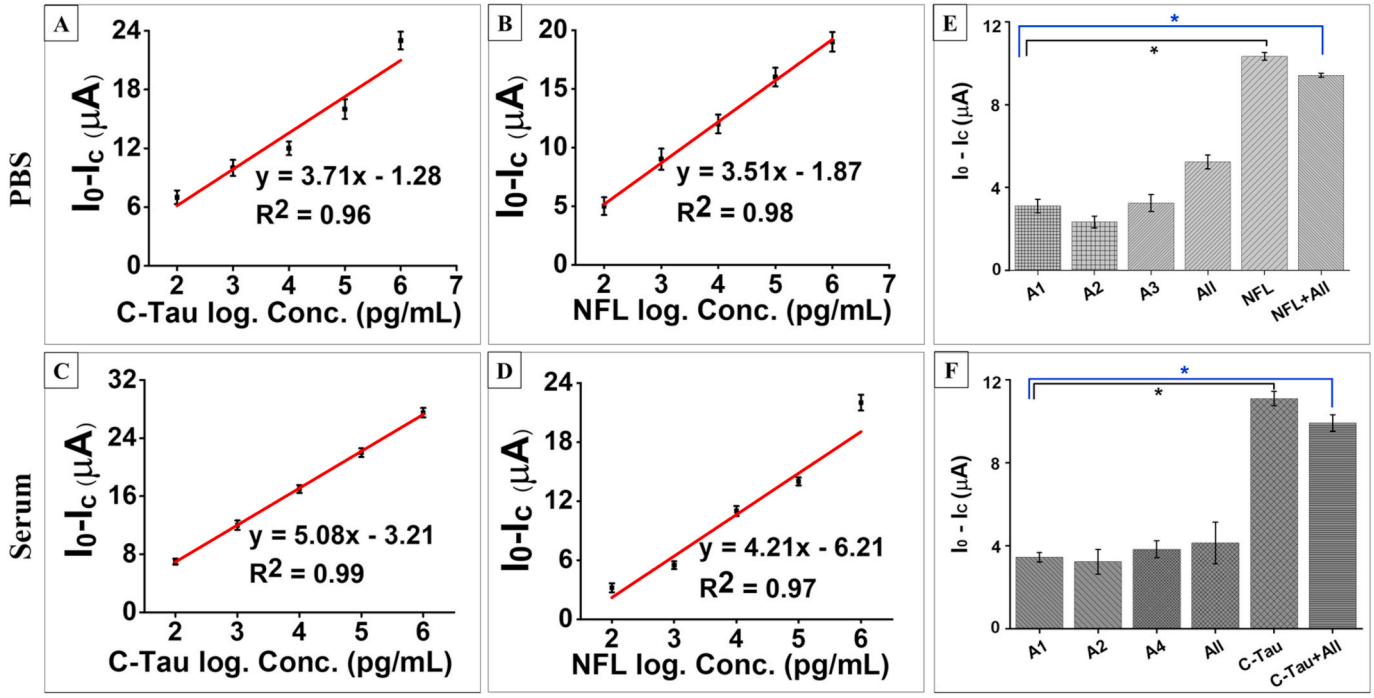

Fig. 3. The linear range and selectivity analysis of the electrochemical C-Tau and NFL immuno-biosensors in PBS and the serum, as measured by μDrop. A linear concentration range of 10 pg/mL – 100 ng/mL detected by immuno-biosensors for (**A**) C-Tau and (**B**) NFL in PBS, and (**C**) C-Tau and (**D**) NFL in the serum. Selectivity assessment of (**E**) NFL, and (**F**) C-Tau immuno-biosensors evaluated by spiking: 1 ng/mL of GABA (A1), UCHL-1(A2), C-Tau (A3), NFL (A4), All (A1-A3/A4), as well as the target analyte with interfering molecules (All) in PBS. All measurements were performed three times (n = 3), and the data is displayed as mean ± SEM ($P < 0.05$).

detection range and LOD (Table S4). The linear response formed the basis of quantifying target analytes' concentration in patient samples.

3.8. Selectivity assessment of the immuno-biosensors

CNS injury can precipitate changes in the concentration of several proteins and neurotransmitters in the blood in addition to C-Tau and NFL(Adrian et al., 2016; North et al., 2012; Yokobori et al., 2015). Here, the selectivity of the immuno-biosensors measured by the μDrop was assessed to characterize the effect of such interfering substances in recording the signals resulting from C-Tau or NFL. The sensors were independently tested with 1 ng/mL of Gamma-aminobutyric acid (GABA) (A1), UCHL-1 (A2), NFL (A3), All (A1, A2, A3), C-Tau (A4), and C-Tau + All to evaluate the selectivity of the developed C-Tau immuno-biosensors (Fig. 3E). The electrical signals directly related to the interfering molecules remain limited to 4 μA, whereas C-Tau and C-Tau + All were above 10 μA. It is noted that the signal recorded due to the interfering molecules was in the same limit as the signal recorded for the BSA-blocking step and 1 pg/mL target analyte concentration, demonstrating the high selectivity of the biosensors for the detection of the target analytes (Fig. 3E).

Similarly, the selectivity of the NFL immuno-biosensors was evaluated in the presence of 1 ng/mL of GABA (A1), UCHL-1 (A2), C-Tau (A4), All (A1, A2, A4), NFL (A3), and NFL + All (Fig. 3F). The signals resulting from the interfering molecules remain within the limit of 1 μA – 2 μA, whereas the signals obtained for NFL and NFL + All were between 11 μA and 12 μA (Fig. 3F). The DPV peak currents did not alter when C-Tau and NFL were measured in samples containing other interfering biomarkers. The highly selective detection highlights the clinical usefulness of these immuno-biosensors and μDrop for detecting C-Tau and NFL targets in the presence of potentially signal interfering analytes.

3.9. Clinical evaluation of the μDrop sensing platform

Based on the performance of the μDrop and immuno-biosensors in detecting CNS biomarkers in the PBS and the serum, we used them for detecting C-Tau and NFL in TBI patients. ELISAs were used to validate the immuno-biosensors and compare the μDrop sensing platform's clinical utility. C-Tau and NFL ELISAs and the immuno-biosensors measured the signal recovery for 50 pg/mL, 100 pg/mL, 500 pg/mL, and 1000 pg/mL concentration of each analyte. ELISAs deliver signal recovery of above 97% for C-Tau and 98% for NFL (Table S5). Similar to ELISAs, the immuno-biosensors' response measured by μDrop delivered the signal recovery of 98% for C-Tau and 94% for NFL (Table S5). The spike recovery comparison between ELISA and the μDrop sensing platform offered a low RSD between the expected and observed signals, in the range of 2.34% – 3.29% and 1.33% – 5.22%, respectively. The results showed that nearly all the concentrations tested were detectable with ELISAs and the immuno-biosensors, further demonstrating the applicability of the developed biosensors and μDrop system for detecting unknown concentrations of C-Tau and NFL in clinical samples. The serum obtained from patients diagnosed with TBI and healthy controls were analyzed with μDrop and the immuno-biosensors to evaluate their ability to detect C-Tau and NFL. Blood was collected within 72 h of injury from six TBI patients admitted to the trauma unit at Foothills Medical Centre, Calgary, Alberta, Canada. Out of 10 clinical samples, 4 were clinical controls (labeled Healthy-1 to Healthy-4), and 6 from patients with TBI (labeled TBI-1 to TBI-6). The severity of the injury is determined based on the Glasgow Coma Score (GSC) (Table 1). GSC score of 15–13 is considered mild, 12–8 is moderate, and less than 8 is severe. All patients have evidence of either focal intracranial bleed, diffuse axonal injury, or both. None of the six patients required intracranial surgery or had any associated injuries, such as musculoskeletal injuries or lung contusion.

The concentration of the biomarker targets in unknown samples was identified based on the detection equation of ELISAs and immuno-biosensors. For ELISAs, absolute values of the unknown C-Tau and NFL concentrations were determined by substituting the absorbance values in their respective ELISA equations. For the immuno-biosensors, the unknown concentration of the target C-Tau and NFL proteins was determined by substituting the absolute peak current (I0 -Ic) in each target's detection equations. All the control samples were found to have C-Tau levels close to the lower end of the detection range of the ELISA method (30.6 pg/mL – 32.2 pg/mL), and the immuno-biosensor (between 10.2 pg/mL – 12.2 pg/mL) (Fig. 4 A, B, Table 1). In the control samples, NFL was measured by ELISA within the range of 30.1 pg/mL – 32.6 pg/mL, and 10.8 pg/mL – 11.7 pg/mL with the biosensor (Fig. 4 A, B, Table 1). The values for all control samples measured were near or below the cut-off concentrations of 70 pg/mL for C-Tau, and 30 pg/mL for NFL (Adrian et al., 2016; North et al., 2012). Therefore, both techniques ruled out the possibility of injury and confirmed the control subjects' healthy state.

Next, serum samples from six clinically confirmed TBI patients were analyzed for C-Tau and NFL levels using ELISA and the immuno-biosensors (Fig. 4 A, B). Comparing the results for TBI patients and healthy controls, a significant correlation ($p = 0.05$; unpaired two-tailed t-test) was observed between C-Tau and NFL measurements (Table 1). Based on the clinical range, the C-Tau immuno-biosensor detected injury in the patient labeled TBI-5, which would have gone undetected with ELISA. C-Tau levels measured using the μDrop did not confirm TBI in the rest of the samples. Four out of the six TBI-samples showed an elevated concentration above the NFL's baseline with both techniques. However, NFL's concentration, which may also indicate severity, was more pronounced with the immuno-biosensor than with the ELISA. This divergent conclusion for the same clinical samples but different biomarkers highlights the gap of the existing techniques in using a single biomarker

Table 1
Concentrations of C-Tau and NFL in clinical samples measured with ELISA and immuno-biosensors.

Sample codes	Demography		Intra-cranial Abnormalities	NFL		C-Tau	
	GCS	Severity	TBI- type	ELISA	Immuno-biosensor	ELISA	Immuno-biosensor
Healthy-1	n/a	n/a	n/a	31.1 ± 0.43	11.21 ± 0.9	30.6 ± 0.32	10.5 ± 0.5
Healthy-2	n/a	n/a	n/a	32.6 ± 0.25	11.72 ± 0.67	30.83 ± 0.65	11.34 ± 0.41
Healthy-3	n/a	n/a	n/a	30.8 ± 0.67	10.74 ± 0.45	31.16 ± 0.53	10.2 ± 0.45
Healthy-4	n/a	n/a	n/a	30.1 ± 0.78	10.85 ± 0.73	32.24 ± 0.32	12.21 ± 0.52
TBI-1	13	Complicated Mild	IH	50.08 ± 0.9	63.08 ± 1.3	34.04 ± 0.8	39.04 ± 1.2
TBI-2	6	Severe	SDH	165.25 ± 1.3	201.25 ± 6.8	55.83 ± 0.93	66.85 ± 2.1
TBI-3	15	Mild	None	31.412 ± 0.43	44.41 ± 1.1	15.61 ± 0.32	22.64 ± 0.9
TBI-4	9	Moderate	SAH	320.89 ± 8.43	351.89 ± 5.7	44.53 ± 0.45	52.53 ± 1.3
TBI-5	6	Severe	SAH	445.06 ± 8.54	491.06 ± 10.2	69.83 ± 0.43	76.83 ± 1.76
TBI-6	15	Complicated Mild	SAH	690.29 ± 9.34	782.29 ± 15.54	40.65 ± 1.2	48.65 ± 1.32

Table 1. Legend: Not applicable (n/a); Mild TBI Glasgow Coma Scale (GCS) 13–15); complicated mild TBI (GCS 13–15 with intracranial lesions); moderate TBI (GCS 8–12); severe TBI (GCS <8). Subarachnoid hemorrhage (SAH), subdural hematoma (SDH), diffuse axonal injury (DAI); intraventricular hemorrhage (IH).

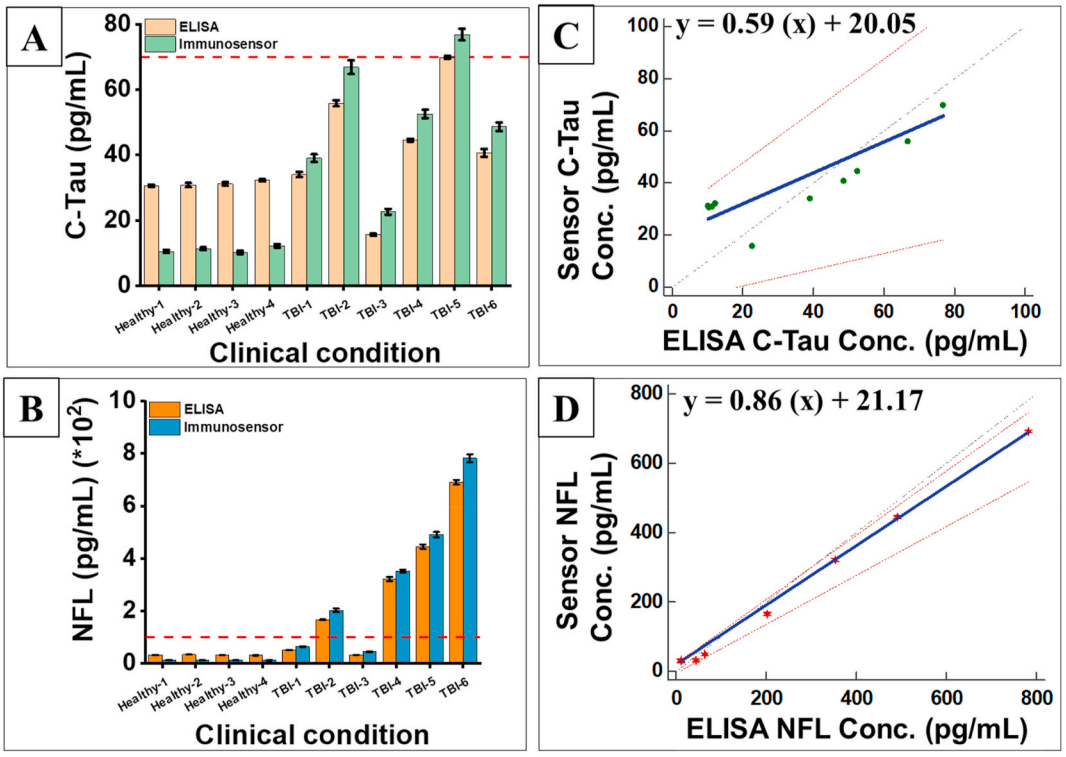

Fig. 4. Evaluation of diagnostic accuracy of the immuno-biosensors in 10 clinical TBI samples and compared with ELISA. (**A**) The concentration of C-Tau obtained with ELISA (orange) and immuno-biosensors (green). (**B**) The concentration of the NFL obtained with ELISA (orange) and immuno-biosensor (blue). The red line indicates the cut-off concentration (baseline). All the samples were measured three times (n = 3) with both the techniques and the data is displayed as mean ± SEM. The diagnostic performance comparison for detecting (**C**) C-Tau, and (**D**) NFL concentrations measured with the μDrop-immunosensors and ELISAs. The regression line is shown solid blue, the dotted black line represents the identity line, and two dashed red lines show the confidence band (n = 10). (For interpretation of the references to colour in this figure legend, the reader is referred to the Web version of this article.)

in blood-based detection and diagnosis of CNS injuries. It is evident that both axon injury biomarkers are expressed differently and have unique concentration profiles, therefore they may not be reliable diagnostic biomarkers if analyzed independently. Therefore, when two targets are considered for the CNS injury diagnosis, ELISA would have only identified elevated NFL concentrations and delivered an inconclusive diagnosis based on C-Tau concentrations. In comparison to ELISA, immunobiosensors conclusively confirmed the injury of TBI-5 using C-Tau concentration.

One of the factors affecting the concentration of biomarkers was intracranial bleeding during the injury (Table 1). The patient sample labeled TBI-6 was diagnosed with mTBI and had intracranial bleeding while displaying a relatively high C-Tau and NFL levels. In contrast, the patient sample labeled TBI-1, diagnosed with mTBI without intracranial bleed, did not show an elevated biomarker concentration. The patient sample TBI-5 with high C-Tau and NFL had presented with a history of other medical issues such as hypertension, high cholesterol, and a remote heart attack while using several medications (Metoprolol, warfarin, Crestor, amlodipine, telmisartan) at the time of injury. These conditions and medicines could have also influenced biomarkers' concentrations.

Passing-Bablock regression (n = 10) was performed to evaluate the performance of the immunosensors in detecting the concentrations of C-Tau and NFL serum samples obtained from clinical TBI patients. Comparing the detection of C-Tau, the values of intercepts A and B were 20.05 (confidence interval (CI), −6.0 to 27.6109) and 0.59 (CI, 0.3159 to 1.00), respectively. The cusum test for linearity showed no significant deviation from linearity with P = 0.06 (Fig. 4C). For NFL, intercepts A and B values were 21.17 (CI, −6.0016 to 23.2027) and 0.8549 (CI, 0.7059 to 0.9229), respectively. The cusum test for linearity showed no significant deviation from linearity with P = 0.77 (Fig. 4D). These statistical analyses suggest that both NFL and C-Tau target proteins were detectable with high confidence with μDrop-immunosensors compared to ELISA.

Receiver operating characteristic (ROC) curve analysis was performed to statistically determine the diagnostic accuracy of the μDrop-biosensors (Fig. S6A,B). Patient cohorts with TBI (n = 6) and control (n = 4), were used, with TBI as a positive state for obtaining the ROC curve. It showed that the μDrop-immuno-biosensors offered 100% sensitivity (AUC = 1) for both the target analytes compared to AUC = 0.83 for NFL and 0.95 for C-Tau by ELISA. Larger AUC and higher specificity and sensitivity obtained for the concentration of targets confirm the superior diagnostic accuracy of the μDrop sensing platform compared to ELISA.

4. Conclusions

We developed the μDrop sensing platform, comprising of electrochemical immuno-biosensors and a low-cost readout system, for the non-invasive quantification of CNS injuries to overcome the diagnostic challenge of CNS injuries. The novel μDrop system was developed with open-source designs and communication protocols to measure C-Tau and NFL levels accurately and reliably in the blood, particularly for TBI patients in a clinical POC setting (Video 1). The combination of μDrop and the immuno-biosensors outperformed several recently reported works (Tables S2, S4), leading to an easy, accessible, fast, reliable, and cost-effective method of testing CNS injuries.

Supplementary video related to this article can be found at https://doi.org/10.1016/j.bios.2021.113033

The technology evaluation strategy of using data from the samples prepared in PBS, the serum, and undiluted clinical samples from TBI patients showed that μDrop offers equally reliable and accurate results as a benchtop potentiostat. Furthermore, μDrop is significantly less

expensive while offering portability and integrated data processing, enhancing its POC use. μDrop offers COVs <5% to operate and perform TBI detection with minimal inputs. This development shows an effective way to eliminate large, expensive, and inaccessible potentiostats for CNS diagnosis, in favor of the portable, accurate, and user-friendly μDrop, which can be directly placed in the hands of healthcare workers in sports medicine or emergency rooms settings.

The device specification allows μDrop to operate for at least one month with a one-time battery charge, rechargeable using a USB cable. The secure communication protocol and data transferability to a cloud server allow for integrating data into the healthcare database. The device is inexpensive to purchase and operate (<$700; Table S1D), with the assay cost <$20 per target. The multiplexing option for μDrop showed that the detection of CNS injuries with two target biomarkers could be more reliable than single biomarker. However, this can be explored further with a larger sample size consisting of spiked, controls, and clinical samples, identifying more accurate and precise biomarkers of injury and recovery. Such an elaborate work can further validate the specificity, sensitivity, and detection rate of the assay and make μDrop and the immune-biosensors useful for non-invasive detection and management of CNS injuries.

Author contributions

Concept and design: S.K, C.D, K.M, A.SN; Experimentation & Data acquisition: S.K, A.SN, B.B, S.B, T.L, K.L, K.S, E.H, R.N; Data analysis and/or interpretation: S.K, A.SN, K.K, A.S, C.D, K.M; Drafting and revising the manuscript: S.K, A.SN, R.N, K.K, A.S, C.D, K.M, A.SN.

#,§: These authors contributed equally to the manuscript.

CRediT authorship contribution statement

Sultan Khetani: Conceptualization, Conception and design of study, Data curation, Funding acquisition, Data acquisition, Formal analysis, Writing - original draft, Drafting the manuscript, Revising the manuscript critically for important intellectual content, Approval of the version of the manuscript to be published. **Anupriya Singh:** Data curation, Funding acquisition, Data acquisition, Formal analysis, Revising the manuscript critically for important intellectual content, Approval of the version of the manuscript to be published. **Brendon Besler:** Data curation, Funding acquisition, Data acquisition, Approval of the version of the manuscript to be published. **Savitri Butterworth:** Data curation, Funding acquisition, Data acquisition, Approval of the version of the manuscript to be published. **Thomas Lijnse:** Data curation, Funding acquisition, Data acquisition, Approval of the version of the manuscript to be published. **Kenneth Loughery:** Data curation, Funding acquisition, Data acquisition, Approval of the version of the manuscript to be published. **Katrin Smith:** Data curation, Funding acquisition, Data acquisition, Approval of the version of the manuscript to be published. **Ehsan Hosseini:** Data curation, Funding acquisition, Data acquisition, Approval of the version of the manuscript to be published. **Rakesh Narang:** Data curation, Funding acquisition, Data acquisition, Revising the manuscript critically for important intellectual content, Approval of the version of the manuscript to be published. **Kunal Karan:** Formal analysis, Approval of the version of the manuscript to be published. **Chantel Debert:** Conceptualization, Conception and design of study, Formal analysis, Revising the manuscript critically for important intellectual content, Approval of the version of the manuscript to be published. **Arindom Sen:** Formal analysis, Revising the manuscript critically for important intellectual content, Approval of the version of the manuscript to be published, Nezhad, Conceptualization, Conception and design of study, Formal analysis, Writing - original draft, Drafting the manuscript, Revising the manuscript critically for important intellectual content, Approval of the version of the manuscript to be published. **Kartikeya Murari:** Conceptualization, and design of study, Formal analysis, Revising the manuscript critically for important intellectual content, Approval of the version of the manuscript to be published.

Declaration of competing interest

The authors declare that they have no known competing financial interests or personal relationships that could have appeared to influence the work reported in this paper.

Acknowledgements

The authors acknowledge Natural Sciences and Engineering Research of Canada (NSERC); Canada Research Chair; Alberta Prion Research Institute (APRI); Alberta Innovates BioSolutions (AIBS); Microsystems Hub, University of Calgary, and CMC – Microsystems, Canada for supporting this research. The Hotchkiss Brain Institute, Canada provided financial support for the collection of blood from the patients with TBI, through a larger study called University of Calgary acute neurorehabilitation initiative. The authors would also like to thank Mark Piitz, Drs. Sean Dukelow, Chester Ho and Patrick Whelan for their help and support in the UCAN study.

Appendix A. Supplementary data

Supplementary data to this article can be found online at https://doi.org/10.1016/j.bios.2021.113033.

References

Adrian, H., Mårten, K., Salla, N., Lasse, V., 2016. Eneuro 3 (6).
Ainla, A., Mousavi, M.P., Tsaloglou, M.-N., Redston, J., Bell, J.G., Fernández-Abedul, M. T., Whitesides, G.M., 2018. Anal. Chem. 90 (10), 6240–6246.
Boulet-Audet, M., Kazarian, S.G., Byrne, B., 2016. Sci. Rep. 6, 30526.
Bruch, R., Baaske, J., Chatelle, C., Meirich, M., Madlener, S., Weber, W., Dincer, C., Urban, G.A., 2019. Adv. Mater. 31 (51), 1905311.
Center, N.S.C.I.S., 2010. The journal of Spinal Cord Medicine 33 (4), 439.
del Río, J.S., Henry, O.Y., Jolly, P., Ingber, D.E., 2019. Nat. Nanotechnol. 14 (12), 1143–1149.
Doolan, A.W., Day, D.D., Maerlender, A.C., Goforth, M., Brolinson, P.G., 2012. Ann. Biomed. Eng. 40 (1), 106–113.
Dryden, M.D., Wheeler, A.R., 2015. PloS One 10 (10) e0140349.
Du, X., Zhang, Z., Zheng, X., Zhang, H., Dong, D., Zhang, Z., Liu, M., Zhou, J., 2020. Nat. Commun. 11 (1), 1–9.
Gill, J., Latour, L., Diaz-Arrastia, R., Motamedi, V., Turtzo, C., Shahim, P., Mondello, S., DeVoto, C., Veras, E., Hanlon, D., 2018. Neurology 91 (15), e1385–e1389.
Gorodkiewicz, E., Ostrowska, H., Sankiewicz, A., 2011. Microchimica Acta 175 (1–2), 177–184.
James, S.L., Theadom, A., Ellenbogen, R.G., Bannick, M.S., Montjoy-Venning, W., Lucchesi, L.R., Abbasi, N., Abdulkader, R., Abraha, H.N., Adsuar, J.C., 2019. Lancet Neurol. 2016 (1), 56–87, 18.
Khetani, S., Aburashed, R., Singh, A., Sen, A., Sanati-Nezhad, A., 2017a. Sensor. Actuator. B Chem. 247, 163–169.
Khetani, S., Kollath, V.O., Eastick, E., Debert, C., Sen, A., Karan, K., Sanati-Nezhad, A., 2019. Biosens. Bioelectron. 111715.
Khetani, S., Kundra, V., Sanati-Nezhad, A., 2017b. CMBES Proceedings 40.
Khetani, S., Mohammadi, M., Nezhad, A.S., 2018a. Biotechnol. Bioeng. 115 (10), 2504–2529.
Khetani, S., Ozhukil Kollath, V., Kundra, V., Nguyen, M.D., Debert, C., Sen, A., Karan, K., Sanati-Nezhad, A., 2018b. ACS Sens. 3 (4), 844–851.
Khetani, S., Yong, K.W., Guan, K., Singh, A., Phani, A., Kollath, V.O., Kim, S., Karan, K., Sen, A., Sanati-Nezhad, A., 2020a. Applied Materials Today 20, 100721.
Khetani, S., Yong, K.W., Ozhukil Kollath, V., Eastick, E., Azarmanesh, M., Karan, K., Sen, A., Sanati-Nezhad, A., 2020b. ACS Appl. Mater. Interfaces 12 (6), 6910–6923.
Langlois, J.A., Rutland-Brown, W., Wald, M.M., 2006. J. Head Trauma Rehabil. 21 (5), 375–378.
Levin, H.S., Diaz-Arrastia, R.R., 2015. Lancet Neurol. 14 (5), 506–517.
Li, J., Li, X.-Y., Feng, D.-F., Pan, D.-C., 2010. Journal of Trauma and Acute Care Surgery 69 (6), 1610–1618.
Mo, J.-W., Ogorevc, B., 2001. Anal. Chem. 73 (6), 1196–1202.
Mohammadian, M., Takala, R., Tenovuo, O., Lagerstedt, L., Ala-Seppälä, H., Frantzén, J., van Gils, M., Hutchinson, P., Katila, A., Maanpää, H.-R., 2019. J. Neurotrauma 36 (10), 1551–1560.
Molina, A., González, J., 2016. Monographs in Electrochemistry.
North, S.H., Shriver-Lake, L.C., Taitt, C.R., Ligler, F.S., 2012. Annu. Rev. Anal. Chem. 5, 35–56.
Organization, W.H., Society, I.S.C., 2013. World Health Organization.

Osteryoung, R., Osteryoung, J., 1981. Philosophical transactions of the Royal Society of London. Series A. Mathematical and Physical Sciences 302 (1468), 315–326.
Peeters, W., van den Brande, R., Polinder, S., Brazinova, A., Steyerberg, E.W., Lingsma, H.F., Maas, A.I., 2015. Acta Neurochir. 157 (10), 1683–1696.
Rao, D.P., McFaull, S., Thompson, W., Jayaraman, G.C., 2017. CMAJ Open 5 (2), E301.
Rowe, A.A., Bonham, A.J., White, R.J., Zimmer, M.P., Yadgar, R.J., Hobza, T.M., Honea, J.W., Ben-Yaacov, I., Plaxco, K.W., 2011. PloS One 6 (9), e23783.
Safavieh, M., Kaul, V., Khetani, S., Singh, A., Dhingra, K., Kanakasabapathy, M.K., Draz, M.S., Memic, A., Kuritzkes, D.R., Shafiee, H., 2017. Nanoscale 9 (5), 1852–1861.
Safavieh, M., Khetani, S., Juillard, F., Kaul, V., Kanakasabapathy, M.K., Kaye, K.M., Shafiee, H., 2016. Biosens. Bioelectron. 80, 230–236.
Salahandish, R., Ghaffarinejad, A., Naghib, S.M., Majidzadeh-A, K., Sanati-Nezhad, A., 2018a. IEEE Sensor. J. 18 (6), 2513–2519.
Salahandish, R., Ghaffarinejad, A., Naghib, S.M., Majidzadeh-A, K., Zargartalebi, H., Sanati-Nezhad, A., 2018b. Biosens. Bioelectron. 117, 104–111.
Salahandish, R., Ghaffarinejad, A., Naghib, S.M., Niyazi, A., Majidzadeh-A, K., Janmaleki, M., Sanati-Nezhad, A., 2019a. Sci. Rep. 9 (1), 1226.
Salahandish, R., Ghaffarinejad, A., Omidinia, E., Zargartalebi, H., Majidzadeh-A, K., Naghib, S.M., Sanati-Nezhad, A., 2018c. Biosens. Bioelectron. 120, 129–136.
Salahandish, R., Zargartalebi, H., Janmaleki, M., Khetani, S., Azarmanesh, M., Ashani, M. M., Aburashed, R., Vatani, M., Ghaffarinejad, A., Sanati-Nezhad, A., 2019b. Advanced Materials Technologies 4 (11), 1900478.
Sha, R., Komori, K., Badhulika, S., 2017. Electrochim. Acta 233, 44–51.
Šimšíková, M., Antalík, M., Kaňuchová, M., Škvarla, J., 2013. Appl. Surf. Sci. 282, 342–347.
Singh, R., Hong, S., Jang, J., 2017. Sci. Rep. 7, 42771.
Valente, K.P., Khetani, S., Kolahchi, A.R., Sanati-Nezhad, A., Suleman, A., Akbari, M., 2017. Drug Discov. Today 22 (11), 1654–1670.
Vedadghavami, A., Minooei, F., Mohammadi, M.H., Khetani, S., Kolahchi, A.R., Mashayekhan, S., Sanati-Nezhad, A., 2017. Acta Biomater. 62, 42–63.
Wang, X., Cohen, L., Wang, J., Walt, D.R., 2018. Journal of the. American Chemical Society 140 (51), 18132–18139.
Xiong, K., Fan, Q., Wu, T., Shi, H., Chen, L., Yan, M., 2017. Mater. Sci. Eng. C 81, 386–392.
Yokobori, S., Zhang, Z., Moghieb, A., Mondello, S., Gajavelli, S., Dietrich, W.D., Bramlett, H., Hayes, R.L., Wang, M., Wang, K.K., 2015. World Neurosurgery 83 (5), 867–878.
Zetterberg, H., Smith, D.H., Blennow, K., 2013. Nat. Rev. Neurol. 9 (4), 201–210.